

UCSF

UC San Francisco Previously Published Works

Title

LC3 and p62 as Diagnostic Markers of Drug-induced Autophagic Vacuolar Cardiomyopathy

Permalink

<https://escholarship.org/uc/item/0r48c9wz>

Journal

The American Journal of Surgical Pathology, 37(7)

ISSN

0147-5185

Authors

Daniels, Brianne H
McComb, Rodney D
Mobley, Bret C
[et al.](#)

Publication Date

2013-07-01

DOI

10.1097/PAS.0b013e3182863fa8

Peer reviewed

This is a non-final version of an article published in the final form in
Am J Surg Pathol 2013; 37(7):1014-21
doi: 10.1097/PAS.0b013e3182863fa8

**LC3 and p62 as diagnostic markers of drug-induced
autophagic vacuolar cardiomyopathy:
A study of three cases**

**Brianne H. Daniels, BA^{1,2}, Rodney D. McComb, MD³, Bret C.
Mobley, MD⁴, S. Humayun Gultekin, MD⁵, Han S. Lee, MD PhD¹,
and Marta Margeta, MD PhD^{1*}**

¹ University of California San Francisco, San Francisco, CA

² Touro University California, Vallejo, CA

³ University of Nebraska Medical Center, Omaha, NE

⁴ Vanderbilt University Medical Center, Nashville, TN

⁵ Oregon Health and Science University, Portland, OR

*Corresponding author:

UCSF Pathology, Box 0511 | 513 Parnassus Ave., HSW-514
San Francisco, CA 94143

Marta.Margeta@ucsf.edu

415-514-0228 (phone) | 415-514-3165 (fax)

Conflicts of Interest and Source of Funding: The study was supported by departmental funds. No conflicts of interest are declared.

ABSTRACT

Autophagic vacuolar cardiomyopathy is an under recognized, but potentially fatal, complication of treatment with chloroquine (CQ) and its derivative hydroxychloroquine (HCQ), which are used as therapy for malaria and common connective tissue disorders. Currently, the diagnosis of autophagic vacuolar cardiomyopathy is established through an endomyocardial biopsy and requires electron microscopy, which is not widely available and has a significant potential for sampling error. Recently, we have reported that immunohistochemistry for autophagic markers LC3 and p62 can replace electron microscopy in the diagnosis of HCQ- and colchicine-induced autophagic vacuolar skeletal myopathies. In the current study, we use three cases of CQ- or HCQ-induced cardiomyopathy and one HCQ-treated control case to show that the same two markers can be used to diagnose autophagic vacuolar cardiomyopathies by light microscopy. CQ- or HCQ-induced autophagic vacuolar cardiomyopathy is not universally fatal, but successful treatment requires early detection. By lowering the barriers to diagnosis, the application of these immunohistochemical markers will decrease the number of misdiagnosed patients, thus increasing the likelihood of favorable clinical outcomes.

KEY WORDS

Autophagy, diagnostic marker, immunohistochemistry, vacuolar cardiomyopathy

INTRODUCTION

Chloroquine (CQ) and its derivative hydroxychloroquine (HCQ) are 4-aminoquinoline compounds that are commonly used for the prevention and/or treatment of malaria and connective tissue disorders such as rheumatoid arthritis and lupus erythematosus¹. Overall, these drugs have a favorable side effect and safety profile; however, development of an autophagic vacuolar cardiomyopathy is an insufficiently recognized, but potentially fatal, complication of CQ or HCQ treatment.

The existing literature on CQ- and HCQ-induced cardiomyopathy mostly consists of single or double case reports; based on a 2007 summary², 11 cases of HCQ cardiotoxicity, 40 cases of CQ cardiotoxicity, and 3 cases of combined HCQ and CQ cardiotoxicity were reported up to that point. Interestingly, the treatment duration and cumulative drug dosage for reported cases spanned months to years of treatment and hundreds to thousands of grams of drug taken², suggesting that other factors (such as genetic predisposition and/or presence of comorbid diseases) play a role in the development of aminoquinoline-induced cardiomyopathy. HCQ is thought to have a more favorable side effect profile than CQ; however, its increased use may lead to a rise in the number of cases of HCQ-induced toxicity^{2,3}.

Both CQ and HCQ accumulate within lysosomes, resulting in lysosomal alkalization¹ and inhibition of lysosomal hydrolytic enzymes; the resulting block in the processing of key immune regulators is thought to lead to the desired anti-inflammatory effects⁴. However, the concomitant inhibition of macroautophagy (a catabolic process constitutively active in all cell types) can lead to the accumulation of cellular debris and misfolded protein aggregates⁵. The abnormal accumulation of insufficiently degraded cellular components in cardiac myocytes can culminate in autophagic vacuolar cardiomyopathy, which clinically manifests with symptoms of chronic heart failure, conduction disorders, and/or restrictive cardiomyopathy^{2,3,6}.

The diagnosis of autophagic vacuolar cardiomyopathy is generally established through an endomyocardial biopsy; however, routine histology shows primarily cardiomyocyte vacuolation that can be misinterpreted as a nonspecific change or an artifact, particularly when the relevant clinical information regarding CQ or HCQ use is lacking. The specific diagnosis can be made through ultrastructural analysis, which shows frequent autophagic vacuoles with myelin figures (seen in all autophagic myopathies) and/or curvilinear bodies (which are relatively specific for CQ and HCQ toxicity)^{1,2,7-9}; however, the utility of electron microscopy is limited by the special

tissue handling requirements, unavailability of electron microscopes in smaller pathology laboratories, relatively long turn-around time, and significant possibility of a sampling error. Hence, the development of a fast and relatively inexpensive immunohistochemical test for autophagic vacuolar cardiomyopathy, which could be performed on any endomyocardial biopsy that shows vacuolar changes, would decrease the number of misdiagnosed cases and thus significantly improve the expected patient outcomes.

Recently, we have reported that immunohistochemistry for autophagic markers LC3 and p62 can replace electron microscopy in the diagnosis of HCQ- and colchicine-induced autophagic vacuolar skeletal myopathies⁷. Here, we use three cases of CQ- or HCQ-induced autophagic vacuolar cardiomyopathy and one HCQ-treated control case to show that the same two markers can be used to diagnose autophagic vacuolar cardiomyopathies by light microscopy.

MATERIALS AND METHODS

Clinicopathologic evaluation

Clinical history, physical examination findings, laboratory and imaging reports, and surgical and autopsy pathology reports were obtained from outpatient and inpatient medical records of Vanderbilt University Medical Center (Patient 1), Oregon Health and Science University (Patient 2), and University of Nebraska Medical Center (Patients 3 and 4). The permission to use tissue for research was covered by autopsy permits signed by the next-of-kin for patients 2, 3, and 4; for patient 1, Vanderbilt University Institutional Review Board waived the informed consent requirement given a minimal potential for harm. No individually identifiable patient data is presented in this report.

Procedures

Electron microscopy. Ultrathin (80 nm) sections of the glutaraldehyde-fixed, Epon-embedded tissue were stained with 2% uranyl acetate. Sections were examined in an FEI Morgagni transmission electron microscope at 60 kV (patient 1) or 70 kV (patient 2), or JEOL 1230 transmission electron microscope at 60 kV (patients 3 and 4). Images were obtained with a

Megaplug camera model ES 4.0 (patient 1), Hamamatsu Digital Camera model C4742-51-12HR (patient 2), or KeenView high resolution digital camera using Soft Imaging Solutions AnalySIS ITEM software (patients 3 and 4).

Immunohistochemistry. Immunoperoxidase staining for LC3 (mouse monoclonal antibody, clone 5F10, Nanotools) and p62/SQSTM1 (guinea pig polyclonal antibody, catalog number GP62-C, Progen Biotechnik) was performed on the FFPE tissue using Ventana Benchmark XT automated slide preparation system at the UCSF Brain Tumor Research Center Tissue Core. Skeletal muscle from a patient with a documented autophagic vacuolar skeletal myopathy was used as a positive control and normal skeletal muscle as a negative control. Tissue sections (4-5 μ m thickness) were deparaffinized (EZ-Prep, Ventana Medical Systems, at 75°C) followed by antigen-retrieval (Cell Conditioning 1, Ventana Medical Systems, at 95-100°C). Antibodies were incubated at room temperature for 2 h, at 1:100 dilutions. Antibody staining was developed using the UltraView Universal DAB detection system (Ventana Medical Systems), and accompanied by hematoxylin counterstain. For comparison, adjacent serial sections were stained with hematoxylin and eosin (H&E). Source and anatomic location of all stained sections is shown in Table 1.

Quantification. Quantification was performed on immunostained sections of FFPE material using a bright-field light microscope. For skeletal muscle samples, we used the approach described previously⁷. For cardiac samples, we modified the protocol slightly to account for the syncytial nature of the myocardium: only cardiomyocytes clearly identifiable as individual cells were included in the final count. Prior to counting, each slide was viewed at low (2x-20x) and high power (40x) to determine whether positive fibers were present scarcely or in abundance. A total of 200 fibers / slide was counted in specimens with abundant positivity, while a total of 600 fibers / slide was counted in specimens with scarce or patchy positivity (to reduce the sampling error). Tissue on the slide was divided into quadrants and randomly selected non-overlapping fields were counted at high power in each quadrant until the total count was reached. The results were recorded as a percentage (the number of positive fibers divided by the total number of fibers counted).

Imaging. Images were taken with a DP72 digital camera on a BX41 bright-field light microscope using cellSens Entry 1.4 software (all by Olympus Corp) and were edited with Adobe Photoshop CS5 Version 12.0.3.

RESULTS

Clinical histories

Patient 1, a 64-year-old woman with a history of rheumatoid arthritis and chronic renal insufficiency, presented with a 3-month history of progressive muscle weakness involving the lower and upper extremities, chronic dyspnea on exertion, lower extremity edema, and an unintentional 60-pound weight loss. The patient's rheumatoid arthritis had been treated with HCQ for 20 years, most recently at 200 mg / day. The evaluation revealed sick sinus syndrome and paroxysmal atrial fibrillation requiring pacemaker placement, slightly elevated creatine phosphokinase (CPK) level (269 U/L), unremarkable infectious and neoplastic work-ups, and a myositis pattern on electromyogram. Based on a clinical diagnosis of polymyositis, the patient was started on prednisone therapy (60 mg / day; tapered to 20 mg / day over 3 weeks); however, her dyspnea, muscle weakness, and lower extremity edema worsened significantly, leading to hospitalization. Diagnostic work-up at this stage demonstrated cardiomegaly and elevated levels of troponin I (5.06 ng/mL), brain natriuretic peptide (>5,000 pg/mL), creatinine (1.89 mg/dL), and CPK (545 U/L). A coronary angiogram was normal, while a 2-D echocardiogram showed restrictive diastolic filling and moderately increased left ventricular wall thickness concerning for an infiltrative process. The patient underwent endomyocardial and left quadriceps femoris biopsies, both of which showed findings of autophagic vacuolar myopathy consistent with HCQ toxicity. HCQ therapy was discontinued, but the patient's general condition deteriorated with altered mental status, declining renal function, and thrombocytopenia; she died as a result of hypoxic respiratory failure two weeks after hospital admission. Clinical features of this case have been described in an earlier report¹⁰.

Patient 2, a 38-year-old woman with a history of ANA-negative discoid lupus erythematosus (treated with chloroquine [500 mg / day] for seven years), presented with dizziness, syncopal

episodes, progressive bilateral extremity weakness, and decreased muscle mass. The evaluation in a community hospital revealed an elevated CPK level (652 U/L); myopathic features on electromyography; and an intermittent high-grade AV block, congestive heart failure, and a dilated non-ischemic cardiomyopathy with abnormal echogenicity suggestive of an infiltrative myocardial disease. A right ventricular biopsy showed interstitial mononuclear inflammation and vacuolar myocardial changes, which were interpreted as artifactual; slides or tissue from this biopsy were not available for review. A rectal biopsy was negative for amyloid deposition. The patient's cardiac condition progressed to third degree AV block; a pacemaker and a defibrillator were placed and amiodarone started. After a transient two week improvement, her cardiac status continued to fluctuate. Two months later, the patient became hypoxic and was admitted to the university hospital, where she died after repeated episodes of cardiorespiratory arrest and resuscitation; chloroquine treatment was discontinued 5 days prior to death. Clinical features of this case have been described in an earlier report¹⁰.

Patient 3, a 55-year-old woman with a history of mixed connective tissue disease associated with Sjogren's syndrome, Raynaud's phenomenon, and mononeuritis multiplex, was referred for evaluation of end-stage liver disease with recurring pleural effusions and ascites; she had been treated with HCQ (400 mg / day) for six years. Evaluation revealed a left pleural effusion, ascites, portal hypertension, esophageal varices, a small nodular liver, and splenomegaly. Serologies for hepatitis B, hepatitis C, and HIV were negative, and the patient's liver failure was attributed to autoimmune hepatitis. In preparation for liver transplantation, cardiac and pulmonary function work-ups were performed and revealed normal function in both systems, with the exception of a moderately impaired diffusion capacity (42% of predicted value). Four months later, the patient underwent orthotopic liver transplantation without complications; HCQ was continued at the pre-transplantation dose. Two weeks after transplantation, recurrence of bilateral pleural effusions, bilateral lower lobe atelectasis, and ascites necessitated repeat thoracentesis and intubation; the patient remained ventilator-dependent during the remainder of her course. Seven weeks after transplantation, she developed progressive renal insufficiency that eventually required dialysis. Brain natriuretic peptide was 1520 pg/mL, and CPK level was 27 U/L. Echocardiogram showed normal left ventricular size and normal systolic function, while the right ventricle was moderately dilated and exhibited a severely depressed ejection fraction. Ten weeks after transplantation, repeat echocardiogram showed dilation and hypertrophy of the right

ventricle with a severely depressed ejection fraction; blood cultures were positive for *Enterococcus faecalis*, and the patient died a few days later.

Patient 4, a 75-year-old woman with a history of hypertension and hyperlipidemia, developed an undifferentiated connective tissue disease consisting of lichenoid dermatitis, alopecia, and arthralgia. Her lab work-up showed positive ANA, anticardiolipin and anti-U1-RNP antibodies, negative rheumatoid factor, and negative DS-DNA, SSA, SSB, SM, Jo-1, and Scl-70 antibodies. She responded to HCQ with resolution of the rash and decreased hair loss, so it was continued at 400 mg / day. Five years later, at age 80, the patient developed an acute inferior myocardial infarction and underwent percutaneous transluminal coronary angioplasty, stenting of the proximal right coronary artery, and balloon angioplasty of the posterior descending coronary artery. During this hospitalization, HCQ therapy was discontinued. Six weeks later, the patient underwent elective coronary artery bypass of the left anterior descending and left diagonal coronary arteries. The procedure was well tolerated and free of immediate complications, but the patient died two weeks later as a result of aortic dissection.

Cardiac pathology

General findings. At autopsy, the hearts of patient 1 and 2 showed biventricular hypertrophy (530 g and 430 g, respectively). The heart of patient 3 (407 g) showed moderate right ventricular hypertrophy and dilatation; the left ventricle was grossly unremarkable. In addition, there was mild coronary artery disease (less than 50% occlusion) and subacute infectious endocarditis involving the mitral valve. The heart of patient 4 (363 g) showed left ventricular hypertrophy and a healed transmural infarct involving the left ventricular free wall. The right coronary artery stent and the saphenous vein graft to the left diagonal artery were patent, while the vein graft to the left anterior descending coronary artery was 50% occluded by a thrombus. In addition, there was dissection of the ascending, transverse, and thoracic segment of the descending aorta.

Features of autophagic vacuolar cardiomyopathy. The hearts of patients 1-3 demonstrated prominent cytoplasmic vacuolation of some (patient 3, Fig. 1G) to nearly all cardiomyocytes (patients 1 and 2; Figs. 1A and 1D); there was no inflammation, no significant variation in cardiomyocyte diameter or nuclear size and shape, and no fibrosis. Ultrastructurally, there was a marked increase in secondary lysosomes containing electron dense material, lamellated

membrane structures, and curvilinear bodies (Supplemental Digital Content, Fig. S1A-C), indicating a disruption in lysosomal function consistent with CQ- or HCQ-induced autophagic vacuolar cardiomyopathy. In contrast, the heart of patient 4 was microscopically unremarkable except for abundant lipofuscin pigment deposition (Fig. 1J) and fibrosis in the healed infarct area (not shown); there was no increase in the number of autophagic vacuoles on electron microscopy, but frequent curvilinear bodies, often in the vicinity of lipofuscin granules, were present (not shown).

LC3 and p62 immunohistochemistry. The hearts of patients 1-3 showed abundant LC3- and p62-immunopositivity, primarily in the form of puncta, coarse clusters, and large aggregates in the vicinity of vacuoles (Fig. 1). In the endomyocardial biopsy specimen from patient 1 (Figs. 1B-C), nearly all cardiomyocytes were LC3- and p62-positive (Table 2). In the autopsy specimen from patient 2, LC3 and p62 staining was patchy at low magnification, with areas of both high (Figs. 1E-F) and low (Supplemental Digital Content, Fig. S2) staining intensity. At high magnification, however, a very high percentage of LC3- and p62-positive fibers was present even in the weakly stained areas (Supplemental Digital Content, Fig. S2), resulting in a high overall degree of positivity for all sections examined (LC3: 80-82.3%, p62: 90-90.3%; Table 2). A similar patchy pattern of staining was seen in the autopsy specimen from patient 3 (Figs. 2H-I), but the overall fraction of positive fibers was lower than in either patient 1 or patient 2 (LC3: 53.2-69.8%, p62: 52.5-65.3%; Table 2). In the autopsy specimen from patient 4, abundant lipofuscin pigment [a type of pigmented autophagic vacuole that accumulates with aging¹¹] showed weak LC3 and p62-positivity (Figs. 1K-L); this background staining was easily distinguishable from the autophagic vacuolar myopathy-associated LC3 and p62 immunopositivity by its distinct green-brown color, perinuclear localization, and well defined spherical shape of the pigment granules. In this specimen, only rare cardiomyocytes demonstrated coarsely punctate LC3 or p62 staining (LC3: 0.3-2.8%, p62: 0.7-1.0%; Table 2), which was not associated with well-developed vacuolar changes.

Skeletal muscle pathology

Features of autophagic vacuolar skeletal myopathy. Like the hearts, skeletal muscle specimens from patients 1-3 showed light microscopic and ultrastructural features of autophagic

vacuolar myopathy including fiber vacuolation (Figs. 2A, 2D and 2G), focal fiber degeneration/regeneration (Fig. 2A), and accumulation of autophagic vacuoles and curvilinear bodies (Supplemental Digital Content, Figs. S1D-F).

LC3 and p62 immunohistochemistry. Skeletal muscles from patients 1-3 (biopsy specimen for patient 1; autopsy specimens for patients 2 and 3) also showed strong LC3 and p62 immunopositivity (Fig. 2). As previously described in our drug-induced autophagic vacuolar myopathy case series⁷, the staining pattern for both LC3 and p62 was coarsely punctate, coalescing around vacuoles or in the fiber center and running in a linear fashion along the longitudinal axis of the fiber (Figs. 2B-C, 2E-F, and 2H-I). Interestingly, in all three patients the fraction of LC3- or p62-positive skeletal muscle fibers was lower than the fraction of LC3- or p62-positive cardiomyocytes (Table 2), but well above the threshold required for diagnosis of autophagic vacuolar myopathy (defined as 16% LC3-positive fibers and/or 12% p62-positive fibers for 100% specificity⁷).

DISCUSSION

Currently, definitive pathologic diagnosis of CQ- or HCQ-induced autophagic vacuolar cardiomyopathy requires electron microscopic identification of well-developed autophagic vacuoles and curvilinear bodies. In this study, we demonstrate that immunohistochemistry for LC3 and/or p62 can be used to detect autophagosome accumulation by light microscopy, thus providing a valuable diagnostic tool that can be used even by pathology laboratories without easy access to an electron microscope.

The four patients included in our study were all women with a history of rheumatologic and/or connective tissue disease who were treated with CQ or HCQ for 5 to 20 years. Patients 1-3 were diagnosed with autophagic vacuolar myopathy either pre- (patient 1) or post-mortem (patients 2 and 3); patient 4 (“drug-treated control”) was treated with HCQ but showed no evidence of vacuolar change in the heart (Fig. 1J). [Of note, HCQ treatment of patient 4 was discontinued 8 weeks prior to death; however, given that CQ and HCQ have a half-life of 40-50 days and can persist in the skin for even longer time periods^{4, 12, 13}, it is reasonable to assume that patient 4 was exposed to a significant level of circulating HCQ at the time of her death – an

assumption supported by the presence of curvilinear bodies in the heart (not shown).] The three patients with autophagic vacuolar cardiomyopathy showed a very high degree of cardiac LC3- and p62-immunopositivity (50-100%; Fig.1 and Table 2); in contrast, only a minimal degree of staining was present in the heart of patient 4 (0-3%; Fig. 1 and Table 2). The number of cases we studied is too small to allow calculation of sensitivity and specificity for different percentages of LC3- and/or p62-immunopositive cardiomyocytes. However, given that almost no cardiomyocytes were LC3- or p62-positive in the HCQ-treated patient with a non-myopathic heart (patient 4), our data indicate that LC3 and/or p62 immunohistochemistry can be used as a qualitative (yes/no) screening test for autophagic vacuolar cardiomyopathy; in cases with borderline immunopositivity, the diagnosis can be confirmed by subsequent electron microscopy.

In the two autopsy cases in our series (patients 2 and 3), the immunopositivity for both LC3 and p62 was patchy, with high and low staining areas often present side-by-side on the same slide (for example, compare Figs. 2D-F to supplemental Fig. S2; both sets of images were taken from the same section of the interventricular septum). High power examination showed that nearly all vacuolated cardiomyocytes were LC3- or p62-positive even in low staining areas, with faint staining the result of a low number of stained puncta, presumably autophagosomes, in each cell (Supplemental Digital Content, Fig. S2). On a small biopsy sample, such low positivity areas could represent a diagnostic challenge; thus, sampling several non-adjacent endomyocardial sites may improve the diagnostic accuracy. Notably, however, the overall fraction of LC3- or p62-positive cardiomyocytes was remarkably similar among different anatomical regions of the same heart (Tables 1 and 2), suggesting that the exact location of the biopsy site is not critical for the diagnosis.

In all three autophagic vacuolar cardiomyopathy cases examined in the current study, the degree of LC3- and p62-immunopositivity was considerably higher in the patients' hearts than in their skeletal muscles (Table 2). (For patient 4, the autopsy was restricted to the heart, lungs, and aorta by the patient's family; thus, skeletal muscle was not available for analysis.) Given that treatment with CQ or HCQ leads to neuromyotoxicity more commonly than cardiotoxicity, this may represent ascertainment bias (mild cardiac involvement may stay asymptomatic and thus unrecognized in non-fatal cases of CQ- or HCQ-toxicity). Nonetheless, all three patients met the diagnostic criteria for autophagic vacuolar skeletal myopathy⁷. Thus, in a CQ- or HCQ-treated

patient with cardiac symptoms and features of autophagic vacuolar myopathy on skeletal muscle biopsy, it would be clinically reasonable to attribute the heart disease to drug toxicity and discontinue the treatment on empirical basis. Definitive diagnosis, however, would require an endomyocardial biopsy. Regardless of the type of tissue sampled, the use of LC3 and/or p62 immunohistochemistry will facilitate the diagnostic process by decreasing the turn-around time, cost, and sampling error associated with ultrastructural studies⁷.

LC3 (or microtubule-associated protein 1 light chain 3) is an autophagy regulatory protein that binds autophagic membranes in its lipidated (LC3-II) form, which is preferentially detected by immunohistochemistry. p62/SQSTM1, an adapter protein that binds LC3-II and targets ubiquitinated protein aggregates for lysosomal degradation, is selectively degraded by autophagy. Thus, accumulation of LC3-II-labeled autophagosomes and/or p62 aggregates is a robust marker of autophagic flux inhibition at any point beyond autophagosome formation¹⁴. However, cardiac autophagosome build-up is not specific for CQ- or HCQ-induced toxicity and can also be observed in inherited autophagic cardiomyopathies such as Danon disease and acid maltase deficiency (Pompe disease)¹⁵. Thus, the clinical context (patient's age, family history, and medication history) has to be taken into account to properly interpret cardiomyocyte vacuolation associated with a high degree of LC3 and/or p62 immunopositivity. In ambiguous cases, however, ultrastructural identification of curvilinear bodies (Supplemental Digital Content, Fig. S1) would corroborate CQ or HCQ toxicity as the cause of autophagy impairment and autophagosome accumulation.

For patients 1 and 2, autophagic vacuolar cardiomyopathy was the sole cause of death. In contrast, patient 3 had several other co-morbid conditions (renal microangiopathy, splenic infarcts, and subacute infectious endocarditis) that contributed to her death. In this context, it is interesting (1) that echocardiography showed evidence of an infiltrative process only in patients 1 and 2, but not in patient 3, and (2) that both cardiomyocyte vacuolation and the degree of LC3 and p62 positivity were significantly higher in the hearts of patients 1 and 2 (80-100% range) than in the heart of patient 3 (50-60% range). These data suggest that the heart has a large functional reserve, with heart failure developing only when almost the entire myocardium develops prominent accumulation of autophagic debris. However, additional work will be

required to establish whether this observation holds true for most cases of autophagic vacuolar cardiomyopathy.

In summary, CQ- or HCQ-induced autophagic vacuolar cardiomyopathy is not universally fatal – cardiac function can sometimes be regained after the drug is discontinued^{1,6} – but early recognition of this complication requires a high degree of clinical suspicion and accurate pathologic diagnosis. In the current study, we show that immunohistochemistry for autophagic markers LC3 and/or p62 can be used to detect myocardial autophagosome accumulation by light microscopy. By lowering the barrier to accurate diagnosis (vacuolar changes seen on routine histology can appear nonspecific and electron microscopy is not always possible), the availability of these immunohistochemical markers will decrease the number of misdiagnosed patients and thus result in significant improvement in health care outcomes.

ACKNOWLEDGMENTS

We thank Mr. King Chu (UCSF Brain Tumor Research Center Tissue Core) for immunohistochemistry support, Ms. Melissa S. Holzapfel and Ms. Karen Bovard (UNMC) for electron microscopy support, Dr. James Atkinson (Vanderbilt Department of Pathology) for images and analysis of cardiac biopsy electron microscopy, Dr. Stanley J. Radio (UNMC) for providing tissue from the UNMC Cardiovascular Registry, and Ms. Christine Lin (UCSF Department of Pathology) for help with figure preparation.

FIGURE LEGENDS

Figure 1. Histology and LC3 and p62 immunohistochemistry in cardiac sections. A, D, G, and J. H&E-stained sections from patient 1 (A), patient 2 (section C2; D), and patient 3 (section C1; G) show prominent vacuolation of nearly all (A and D) or a subset of cardiomyocytes (G). In contrast, no vacuolation is seen on the H&E-stained section from patient 4 (section C2; J). **B, E, H, and K.** LC3 staining highlights fine to coarse puncta and larger aggregates associated with vacuoles in sections from patients 1-3 (B, E, and H); no staining (except for lipofuscin pigment)

is seen in the section from patient 4 (K). **C, F, I, and L.** p62 immunohistochemistry shows an essentially identical staining pattern. Scale bar, 40 μ M.

Figure 2. Histology and LC3 and p62 immunohistochemistry in skeletal muscle sections. A, D, and G. H&E-stained sections from patient 1 (A), patient 2 (section S1; D), and patient 3 (G) show degenerating/regenerating muscle fibers (A) and mild (A, D) to prominent (G) fiber vacuolation. **B-C, E-F, and H-I.** LC3 and p62 staining is finely to coarsely punctate, associated with vacuoles, and most often localized in the fiber center, aligned with the longitudinal fiber axis. Scale bar, 100 μ M.

Supplemental Digital Content, Figure S1. Ultrastructural findings of autophagic vacuolar myopathy. In both heart (A-C) and skeletal muscle (D-F) preparations, electron microscopy showed accumulation of autophagic vacuoles (secondary lysosomes containing electron-dense material, myelin figures, and organelle remnants), some of which also contained curvilinear bodies (C, E and F). Panel A is from patient 1, panel D from patient 2, and panels B, C, E, and F from patient 3. Scale bars, 3 μ M.

Supplemental Digital Content, Figure S2. Areas of low LC3 and p62 immunopositivity. In some areas, cardiomyocytes showed prominent vacuolation (panels A and B) but a relatively low degree of LC3 and p62 immunopositivity (panels C and E). High power images (panels D and F) show that most vacuolated cardiomyocytes are LC3- or p62-positive, but that there is accumulation of a smaller number of LC3- or p62-labeled autophagosomes per cardiomyocyte than in high positivity areas (compare with Figs. 1E-F, which were taken from the same tissue section). Patient 2, section C2. Scale bars: 100 μ M, panels A, C, and E; 40 μ M, panels B, D, and F.

LIST OF SUPPLEMENTAL DIGITAL CONTENT

Supplemental Digital Content 1.tif

Supplemental Digital Content 2.tif

REFERENCES

1. Estes ML, Ewing-Wilson D, Chou SM, et al. Chloroquine neuromyotoxicity. Clinical and pathologic perspective. *Am J Med.* 1987;82:447-455.
2. Soong TR, Barouch LA, Champion HC, et al. New clinical and ultrastructural findings in hydroxychloroquine-induced cardiomyopathy--a report of 2 cases. *Hum Pathol.* 2007;38:1858-1863.
3. Costedoat-Chalumeau N, Hulot JS, Amoura Z, et al. Cardiomyopathy related to antimalarial therapy with illustrative case report. *Cardiology.* 2007;107:73-80.
4. Fox RI. Mechanism of action of hydroxychloroquine as an antirheumatic drug. *Semin Arthritis Rheum.* 1993;23:82-91.
5. Levine B, Kroemer G. Autophagy in the pathogenesis of disease. *Cell.* 2008;132:27-42.
6. Cotroneo J, Sleik KM, Rene Rodriguez E, et al. Hydroxychloroquine-induced restrictive cardiomyopathy. *Eur J Echocardiogr.* 2007;8:247-251.
7. Lee HS, Daniels BH, Salas E, et al. Clinical utility of LC3 and p62 immunohistochemistry in diagnosis of drug-induced autophagic vacuolar myopathies: a case-control study. *PLoS One.* 2012;7:e36221.
8. Ratliff NB, Estes ML, Myles JL, et al. Diagnosis of chloroquine cardiomyopathy by endomyocardial biopsy. *N Engl J Med.* 1987;316:191-193.
9. Stein M, Bell MJ, Ang LC. Hydroxychloroquine neuromyotoxicity. *J Rheumatol.* 2000;27:2927-2931.
10. Azimian M, Gultekin SH, Hata JL, et al. Fatal antimalarial-induced cardiomyopathy: Report of two cases. *J Clin Rheumatol.* 2012;18:363-366.
11. Sulzer D, Mosharov E, Talloczy Z, et al. Neuronal pigmented autophagic vacuoles: lipofuscin, neuromelanin, and ceroid as macroautophagic responses during aging and disease. *J Neurochem.* 2008;106:24-36.
12. Furst DE. Pharmacokinetics of hydroxychloroquine and chloroquine during treatment of rheumatic diseases. *Lupus.* 1996;5 Suppl 1:S11-15.
13. Mackenzie AH. Pharmacologic actions of 4-aminoquinoline compounds. *Am J Med.* 1983;75:5-10.
14. Klionsky DJ, Abeliovich H, Agostinis P, et al. Guidelines for the use and interpretation of assays for monitoring autophagy in higher eukaryotes. *Autophagy.* 2008;4:151-175.
15. Malicdan MC, Noguchi S, Nonaka I, et al. Lysosomal myopathies: an excessive build-up in autophagosomes is too much to handle. *Neuromuscul Disord.* 2008;18:521-529.

Table 1: Tissue section source and location.

	Heart	Skeletal muscle
Patient 1 (biopsies)	Right ventricle	Quadriceps femoris
Patient 2 (autopsy)	C1: Left ventricle C2: Interventricular septum	S1: Lower rectus S2: Quadriceps femoris S3: Deltoid
Patient 3 (autopsy)	C1: Ventricular septum and posterior RV free wall at the papillary muscle level C2: Posterior LV free wall and ventricular septum at the mid- heart level	Skeletal muscle, not otherwise specified
Patient 4 (autopsy)	C1: Transverse ventricular septum C2: Anterior LV free wall C3: Posterior RV free wall	Not available*

Abbreviations: LV, left ventricle; RV, right ventricle.

* Skeletal muscle was not available for patient 4, whose autopsy was restricted by the patient's family to the heart, lungs, and aorta.

Table 2. Quantification of LC3 and p62 immunopositivity.

	Heart		Skeletal muscle	
	LC3	p62	LC3	p62
Patient 1	98.5%	98.5%	36.0%	43.5%
Patient 2	C1: 80.0% C2: 82.3%	C1: 90.3% C2: 90.0%	S1: 59.0% S2: 67.0% S3: 85.0%	S1: 65.5% S2: 73.5% S3: 87.5%
Patient 3	C1: 53.2% C2: 69.8%	C1: 52.5% C2: 65.3%	46.5%	31.5%
Patient 4 (control)	C1: 2.8% C2: 2.2% C3: 0.3%	C1: 1.0% C2: 0.7% C3: 1.0%	Not available	Not available

Localization of individual tissue sections is shown in Table 1. For patient 3, each cardiac section included two different anatomic areas (C1: RV and septum; C2: LV and septum), both of which showed a similar degree of LC3 and p62 labeling; the percentages shown in the table are averages for all tissue on the slide. Skeletal muscle LC3 and p62 labeling could not be evaluated for patient 4, whose autopsy was restricted by the patient's family to the heart, lungs, and aorta.

Figure 1

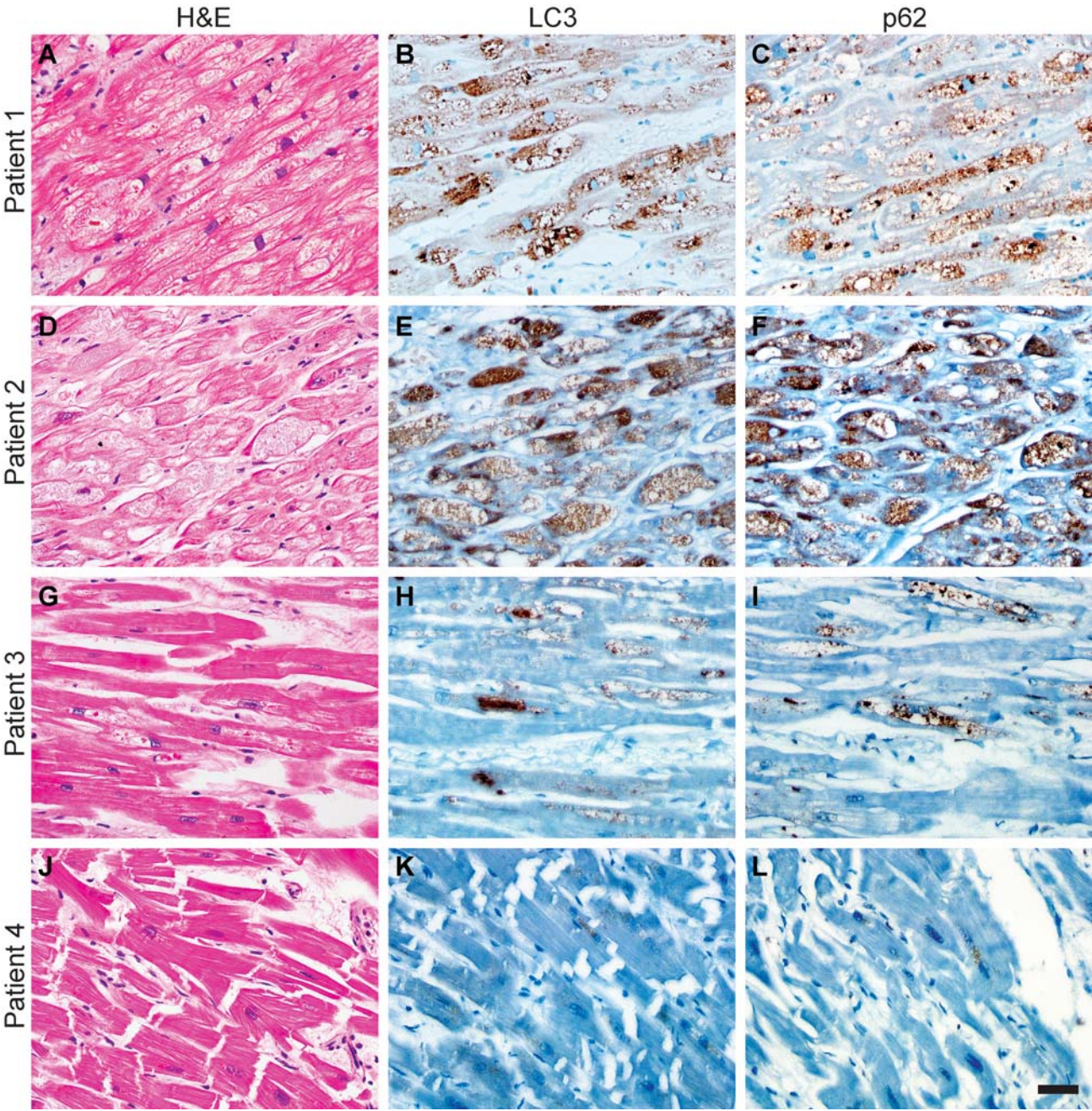
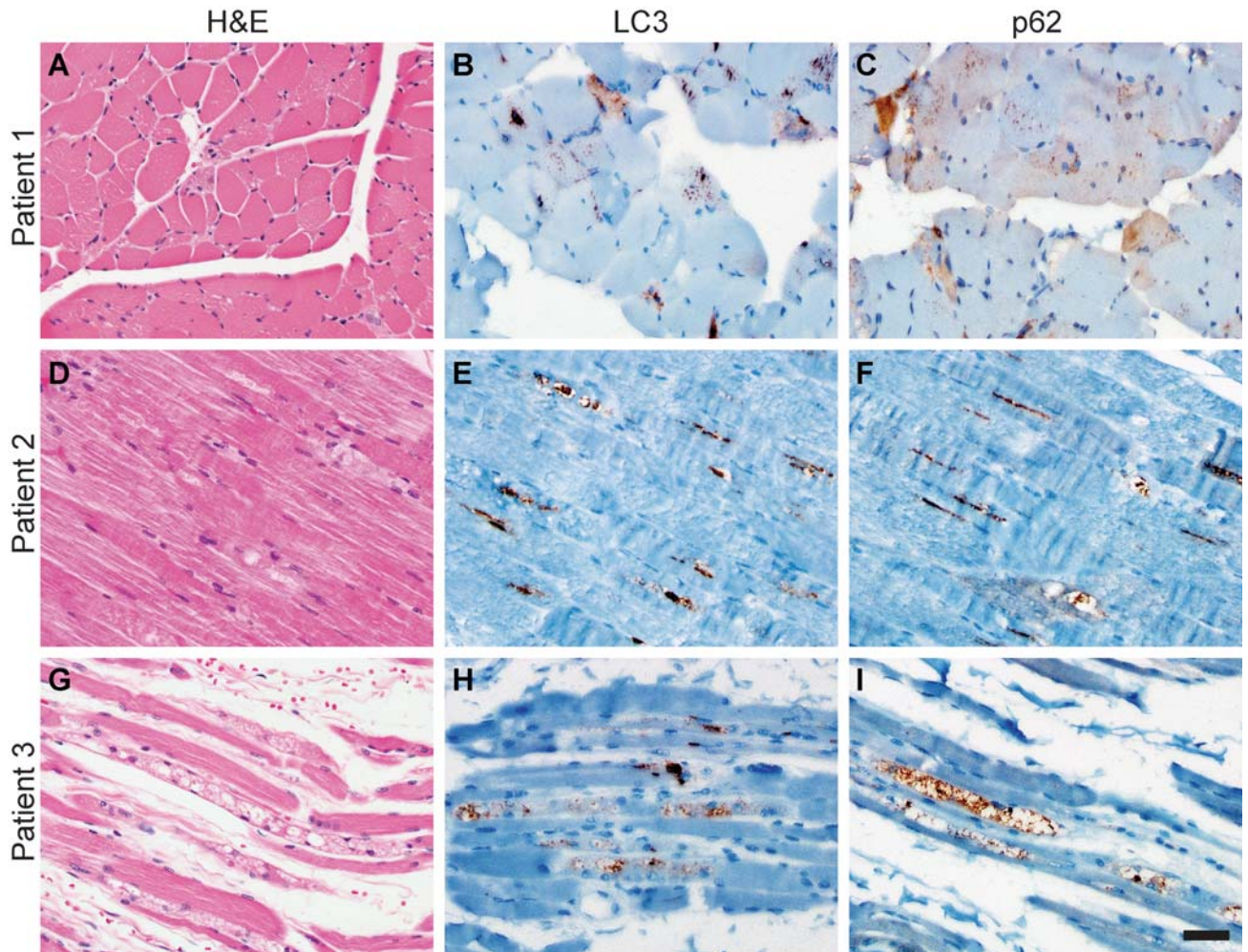
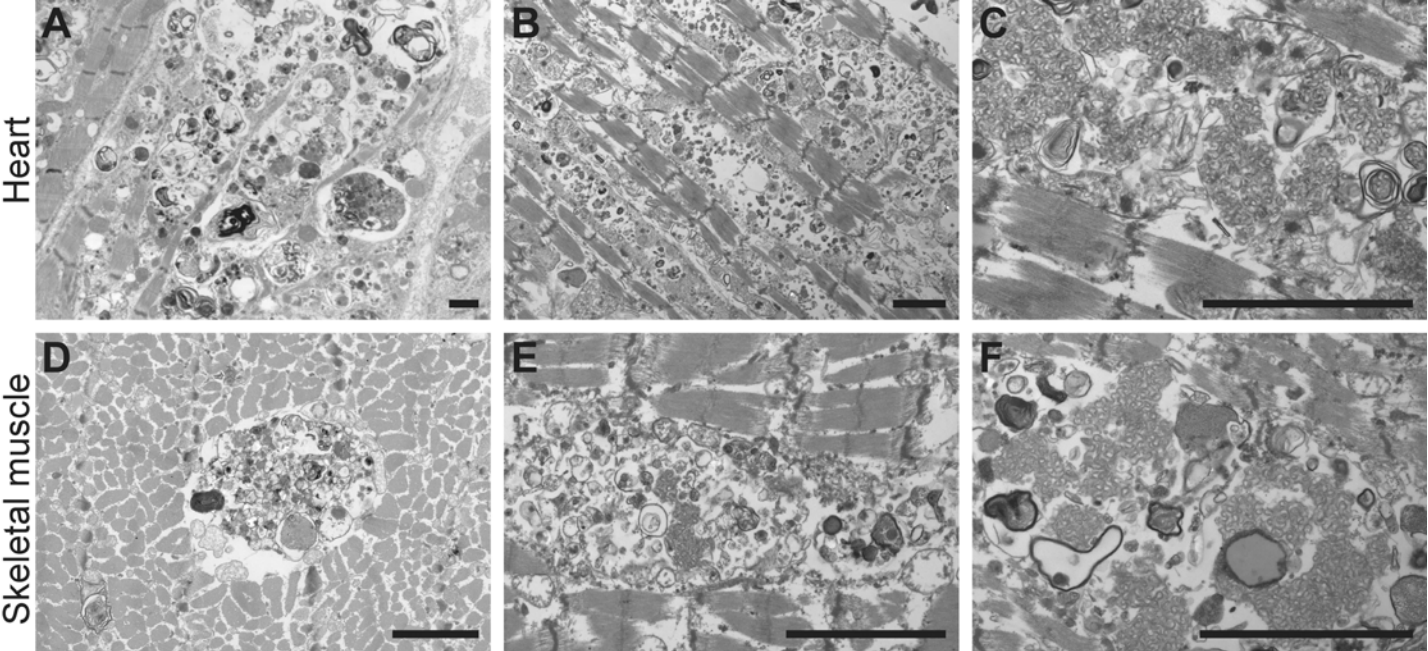


Figure 2



Supplemental Digital Content 1



Supplemental Digital Content 2

